Nuclear Instruments and Methods in Physics Research A 338 (1994) 442–446
North-Holland

NUCLEAR INSTRUMENTS & METHODS IN PHYSICS RESEARCH
Section A

An alternative method for computing the influence of multiphonon processes in the inelastic scattering of neutrons
Application to metal hydrides

J. Mestnik Filho, J.I. Moura

Instituto de Pesquisas Energéticas e Nucleares, IPEN-CNEN/SP, Cx.Postal 11049, 05422-970 São Paulo, SP, Brazil

(Received 30 December 1992; revised form received 26 August 1993)

An alternative method for calculating the multiphonon contribution to the inelastic scattering of neutrons, which is not based on phonon expansion, is presented. The method has been applied to a metal hydride system possessing two hydrogen vibration frequency bands.

1. Introduction

During the last years the inelastic incoherent neutron scattering (IINS) technique has been progressively applied in the study of molecular dynamics. In particular the technique has been used to study the metal-hydrogen systems and hydrocarbon crystals due to the relatively large neutron scattering cross section of hydrogen. In an IINS experiment the distribution of vibration frequencies $g(\omega)$ can be determined by measuring the energy exchange between the neutrons and the system under study. More precisely, in the one phonon approach in which only one quantum of the vibrational energy of one normal mode is exchanged with a neutron, the spectrum of inelastically scattered neutrons is directly related to the $g(\omega)$ weighted by the squares of the amplitudes of atomic vibrations. This can be reduced to $g(\omega)$ in systems with cubic symmetry.

It is known however that it is not possible to avoid the so called multiphonon processes in an inelastic neutron scattering experiment [1,2]. For these processes more than one phonon from one or more modes are exchanged with the neutron. To minimize these effects the measurements must be carried out at low temperatures and at low magnitude of the scattering vector $\boldsymbol{Q}$. However the later condition (low $\boldsymbol{Q}$) is difficult to attain in practice, specially when one attempts to determine the high energy modes as the optical modes in metal hydrides. Moreover some experiments have been carried out recently at large values of $\boldsymbol{Q}$ in order to study the anharmonicity of hydrogen potential well in metal hydrides [3].

In this context, the calculation of the inelastic neutron scattering cross sections which takes into account the multiple phonon processes is desirable, and has been the subject of a recent investigation [1]. The usual way to treat this problem is to expand the expression for the differential scattering cross section of neutrons in a power series, each term of the series being related to a respective number of phonons involved in the inelastic scattering [1,2].

In the present work we report an alternative method to calculate the multiphonon contribution which is not based on phonon expansion but on a numerical Fourier transformation of the corresponding intermediate scattering function evaluated on the basis of a model frequency spectrum. The method is applied to a simple metal hydride characterized by a hydrogen frequency distribution with two bands: a Debye spectrum and a well separated localized mode represented by a Gaussian function. The method however, can also be applied to more complex systems after solving specific dynamic models.

2. Outline of the method

The general expression for the differential incoherent inelastic scattering cross section of neutrons is given by ref. [4, Eqs. (4.86) and (4.87)]:

$$\frac{\partial^2\sigma}{\partial\Omega\partial\omega} = \frac{N}{4\pi}\frac{k}{k_0}\frac{1}{2\pi}\int_{-\infty}^{\infty} \mathrm{d}t \exp(-\mathrm{i}\omega t) \times \sum_d \sigma^d_{\mathrm{incoh}} \exp\left(-2W_d(\boldsymbol{Q})\right) \times \{\exp\left(\gamma_d(t)\right) - 1\}\,, \tag{1}$$

where the function $\gamma_d(t)$ is given by:

$$\gamma_d(t) = \frac{\hbar}{2NM_d}\sum_{j\boldsymbol{q}} \frac{|\boldsymbol{Q}\cdot\boldsymbol{e}^d_j(\boldsymbol{q})|^2}{\omega_j(\boldsymbol{q})} \times \{[n_j(\boldsymbol{q})+1]\exp(\mathrm{i}\omega_j(\boldsymbol{q})t) + n_j(\boldsymbol{q})\exp(-\mathrm{i}\omega_j(\boldsymbol{q})t)\}\,. \tag{2}$$

In these expressions, d is an index which runs over the different nuclei in a unit cell, σ^d_{incoh} is the incoherent scattering cross section for the nucleus d and M_d stands for its mass; $\boldsymbol{e}^d_j(\boldsymbol{q})$ is the polarization vector of a normal mode with wave vector $\boldsymbol{q}$ from branch j due to the nucleus d. N is the number of unit cells, $\hbar$ is the Planck constant divided by 2π and $n_j(\boldsymbol{q})$ is the Bose occupation number for the mode $(j,\boldsymbol{q})$ with frequency $\omega_j(\boldsymbol{q})$ which is given by $n_j(\boldsymbol{q}) = \{\exp(\hbar\omega_j(\boldsymbol{q})/KT) - 1\}^{-1}$, where K is the Boltzman constant and T the absolute temperature. As usual, $\boldsymbol{k}$ and $\boldsymbol{k}_0$ are respectively the initial and final neutron wave vectors, $\hbar\omega = E_i - E_f$ is the energy transferred to the normal modes where E_i and E_f are respectively the initial and final neutron energies. The Debye–Waller factor $\exp(-2W_d(\boldsymbol{Q}))$ can be determined from $2W_d(\boldsymbol{Q}) = \gamma_d(0)$. The Eq. (1) is exact within the harmonic approximation of the lattice vibrations [4, p. 82].

The one phonon approach to the scattering cross section is obtained after expansion of the term in braces in Eq. (1) and retaining only the first order term:

$$\exp(\gamma_d(t)) - 1 \sim \gamma_d(t)\,. \tag{3}$$

Applying the above approximation in Eq. (1) and performing the Fourier transformation, the following well known expression for one phonon scattering cross section is obtained:

$$\frac{\partial^2\sigma}{\partial\Omega\partial\omega} = \frac{N}{4\pi}\frac{k}{k_0}\sum_d \sigma^d_{\text{incoh}}\exp(-2W_d(\boldsymbol{Q})) \times \frac{\hbar}{2NM_d}\sum_{j\boldsymbol{q}}\frac{|\boldsymbol{Q}\cdot\boldsymbol{e}^d_j(\boldsymbol{q})|^2}{\omega_j(\boldsymbol{q})} \times \{[n_j(\boldsymbol{q})+1]\,\delta(\omega-\omega_j(\boldsymbol{q})) + n_j(\boldsymbol{q})\delta(\omega+\omega_j(\boldsymbol{q}))\}\,. \tag{4}$$

Comparing Eq. (2) with the last term in Eq. (4) it can be seen that after the Fourier transformation, a delta function in the frequency domain is generated for each corresponding periodic function in the time domain contained in $\gamma_d(t)$. The summation of these delta functions over the $(j,\boldsymbol{q})$ space generates the frequency spectrum.

It is interesting to see how this spectrum is modified when Eq. (1) is calculated exactly. The $\exp(\gamma_d(t))$ term implies an exponentiation of a sum of periodic functions and has the effect of deforming these functions in a way that generates a whole series of harmonics for each individual frequency as well as all combinations of sums and differences between these frequencies. The derived spectrum after the Fourier transformation of such a distorted sum of periodic functions will obviously contain the one phonon and all the higher order phonon contributions.

To perform such calculation in practice, it is convenient to rewrite the term in braces in Eq. (1) and separate it in its real and imaginary components:

$$A^d(\boldsymbol{Q},t) = \text{Re}\{\exp(\gamma_d(t)) - 1\} = \exp\left\{\frac{\hbar^2Q^2}{2M_n}G^d_s(t)\right\} \times \cos\left\{\frac{\hbar^2Q^2}{2M_n}G^d_a(t)\right\} - 1\,, \tag{5}$$

$$B^d(\boldsymbol{Q},t) = \text{Im}\{\exp(\gamma_d(t)) - 1\} = \exp\left\{\frac{\hbar^2Q^2}{2M_n}G^d_s(t)\right\} \times \sin\left\{\frac{\hbar^2Q^2}{2M_n}G^d_a(t)\right\}, \tag{6}$$

with the definitions:

$$G^d_s(t) = \frac{1}{N}\sum_{j,\boldsymbol{q}}\frac{M_n}{M_d}\left|\hat{\boldsymbol{Q}}\cdot\boldsymbol{e}^d_j(\boldsymbol{q})\right|^2 \times \frac{[1+2n_j(\boldsymbol{q})]\cos(\omega_j(\boldsymbol{q})t)}{\hbar\omega_j(\boldsymbol{q})}\,, \tag{7}$$

$$G^d_a(t) = \frac{1}{N}\sum_{j,\boldsymbol{q}}\frac{M_n}{M_d}\left|\hat{\boldsymbol{Q}}\cdot\boldsymbol{e}^d_j(\boldsymbol{q})\right|^2\frac{\sin(\omega_j(\boldsymbol{q})t)}{\hbar\omega_j(\boldsymbol{q})}\,, \tag{8}$$

In these expressions M_n is the neutron mass and $\hat{\boldsymbol{Q}}$ is a unit vector along the $\boldsymbol{Q}$ direction. The subscripts s and a stand respectively for symmetric and anti symmetric character relative to time reversal. $A^d(\boldsymbol{Q},t)$ and $B^d(\boldsymbol{Q},t)$ are implicit functions of the energy transfer $\hbar\omega$ due to the kinematic factor:

$$\frac{\hbar^2Q^2}{2M_n} = (\hbar\omega + 2E_{i,f}) - 2\,[(\hbar\omega + E_{i,f})E_{i,f}]^{1/2}\cos(\theta)\,, \tag{9}$$

where $E_{i,f}$ is the initial or the final neutron energy respectively for neutron energy gain or neutron energy loss experiments, while θ is the scattering angle. The cross section is obtained by performing the real part of the Fourier integration (the imaginary part is always zero):

$$\frac{\partial^2\sigma}{\partial\Omega\partial\omega} = \frac{N}{4\pi}\frac{k}{k_0}\sum_d\sigma^d_{\text{incoh}}\exp(-2W_d(\boldsymbol{Q})) \times \frac{1}{2\pi}\left\{\int dt\cos(\omega t)A^d(\boldsymbol{Q},t) \pm \int dt\sin(\omega t)B^d(\boldsymbol{Q},t)\right\} \tag{10}$$

The plus and minus signs in Eq. (10) correspond to neutron energy loss and neutron energy gain respectively, according to the experiment, while ω is as-

sumed to be positive in both cases. In the present notation the intermediate scattering function for a given nucleus d is:

$$I^d(\boldsymbol{Q},t) = \left\{A^d(\boldsymbol{Q},t) + \mathrm{i}B^d(\boldsymbol{Q},t)\right\} \times \exp\left(-2W_d(\boldsymbol{Q})\right) . \quad (11)$$

The corresponding scattering law is given by:

$$S^d(\boldsymbol{Q},\omega) = \int \mathrm{d}t \exp(-\mathrm{i}\omega t) I^d(\boldsymbol{Q},t) . \quad (12)$$

In terms of which the cross section is:

$$\frac{\partial^2\sigma}{\partial\Omega\partial\omega} = \frac{N}{4\pi}\frac{k}{k_0}\sum_d \sigma^d_{\mathrm{incoh}} S^d(\boldsymbol{Q},\omega) . \quad (13)$$

The Eq. (10) is exact since it is derived from Eq. (1). The scattering law in Eq. (12) satisfies the condition of detailed balance and its first moment gives the recoil energy of the target system, as expected. These properties are easily verified directly from Eq. (1) after replacing t by $-t + \mathrm{i}\hbar/KT$ (detailed balance condition) or performing the time derivative $\mathrm{i}\hbar(\partial/\partial t)$ at $t = 0$ (recoil energy) [4, pp. 45–50].

3. Application of the method

In order to apply the Fourier transformation method to evaluate the inelastic scattering cross section for neutrons, the functions $G^d_s(t)$ and $G^d_a(t)$ must be defined. They can be obtained, in principle, after solving a particular dynamic model where the eigenvectors $\boldsymbol{e}^d_j(\boldsymbol{q})$ and the eigenfrequencies $\omega_j(\boldsymbol{q})$ are derived as a function of the force constants between the atoms. Although this procedure is not simple, Kolesnikov et al. [1] have performed such calculations for relatively complex systems. Here we will restrict ourselves to the case of a typical metal–hydrogen system for which one can assume a phenomenological density of frequencies.

The term $|\hat{\boldsymbol{Q}}\cdot\boldsymbol{e}^d_j(\boldsymbol{q})|^2$ in Eqs. (7) and (8) is replaced by the mean value 1/3 which is valid for crystals with cubic symmetry, and is expected to be a good approximation even for less symmetric systems in policrystalline substances. Thus the summation over the modes $(j,\boldsymbol{q})$ can be replaced by an integral over frequencies ω':

$$G^d_s(t) = \int \mathrm{d}\omega' Z^d(\omega') \frac{[1 + 2n(\omega')]\cos(\omega' t)}{\hbar\omega'} , \quad (14)$$

$$G^d_a(t) = \int \mathrm{d}\omega' Z^d(\omega') \frac{\sin(\omega' t)}{\hbar\omega'} , \quad (15)$$

Only one kind of atoms is considered, i.e., hydrogen atoms. The frequency spectrum $Z^{\mathrm{H}}(\omega')$ for a hydrogen atom in a metal–hydride is approximated by:

$$Z^{\mathrm{H}}(\omega') = \mu\frac{3\omega'^2}{\omega_D^3} + \frac{1-\mu}{\sqrt{2\pi}\sigma}\exp\left(-\frac{(\omega_0-\omega')^2}{2\sigma^2}\right) , \quad (16)$$

which is a Debye spectrum for the band modes of hydrogen vibrations plus a Gaussian shaped spectrum for the localized modes. In Eq. (16), ω_0 is the local mode frequency while σ is the standard deviation around ω_0. ω_D is the Debye cut-off frequency and μ is equal to $M_{\mathrm{H}}/(M_{\mathrm{H}} + M_{\mathrm{M}})$ where M_{H} and M_M are respectively the hydrogen and the metallic atoms masses. The normalization of the model frequency spectrum (16) with respect to the above mass ratio is necessary to compensate for the similar mass ratio present in Eqs. (7) and (8). This reflects the dependence of the scattering cross section on the square of the amplitudes of atomic vibrations. Here it was assumed that the neutron and proton masses are equal and also that the hydrogen vibration amplitude is the same as that of the metallic atoms at low frequencies. As the hydrogen to metal and the metal to metal force constants seem to be nearly equal [5], the ratio between ω_0 and the mean frequency of the band modes should be roughly equal to $(M_{\mathrm{M}}/M_{\mathrm{H}})^{1/2}$.

Once the model density of states has been established, the inelastic scattering cross section for neutrons can be computed through the Eqs. (14) and (15), (5) and (6), and (10). It should be noticed that there is no need for the Schofield [6,4, sect. 3.4] approximation to be considered since the auto-correlation function (corresponding to the model frequency spectrum) is implicitly computed in an exact way. This auto-correlation function can otherwise be explicitly calculated through the *spatial* Fourier transform of Eq. (11).

4. Results and discussion

The plots of the relative neutron intensity as a function of the energy transfer for a neutron energy loss experiment are shown in Figs. 1–4. To convert to scattering cross sections, the vertical scales of the plots must be multiplied by $(N/4\pi)(k/k_0)(\sigma^{\mathrm{H}}_{\mathrm{incoh}})$. The following parameters values were chosen as representative of a typical metal hydride [7]: $\hbar\omega_0 = 127$ meV, $\beta = 2.35\sigma = 10$ meV (β is the full width at a half maximum (FWHM) of the localized frequencies distribution), $\omega_D = 30$ meV, $\mu = 0.04$, $T = 15$ K, $\theta = 90$ degrees and $E_f = 4$ meV. Each one of the Figs. 1–4 presents the results for three values of one of these parameters, while the other parameters are kept fixed. No instrumental resolution effects have been taken into account. In these figures the shaded areas are due

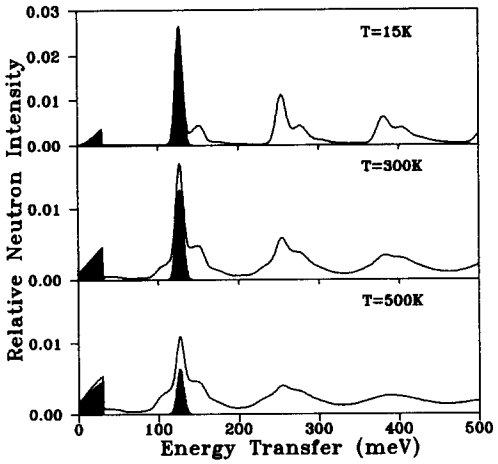

Fig. 1. Calculated relative neutron intensity as a function of the energy transfer in a neutron energy loss scattering experiment with metal hydride for various temperatures. Shaded areas: one phonon scattering. Line: all phonon scattering. $\hbar\omega_0 = 127$ meV, $\omega_D = 30$ meV, $\beta = 10$ meV, $\mu = 0.04$, $E_f = 4$ meV.

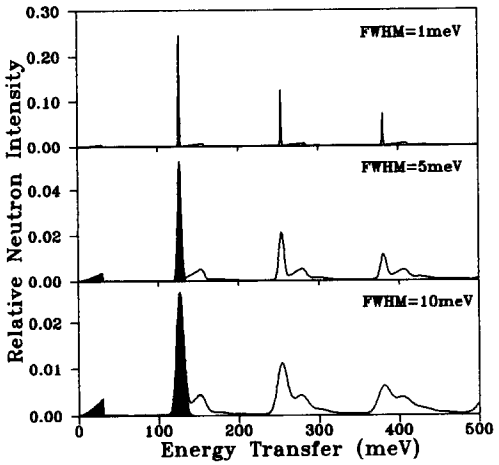

Fig. 2. Calculated relative neutron intensity as a function of the energy transfer in a neutron energy loss scattering experiment with metal hydride for various widths of the localized hydrogen vibrations. Shaded areas: one phonon scattering. Line: all phonon scattering. $\hbar\omega_0 = 127$ meV, $\omega_D = 30$ meV, $T = 15$ K, $\mu = 0.04$, $E_f = 4$ meV.

to one phonon scattering processes whereas the lines represent the results for the all phonon contributions.

As can be seen, the higher order phonon scattering appears mainly as side bands around the localized frequency peak at the fundamental transition as well as at the higher harmonics $\hbar\omega = 2\hbar\omega_0$, $\hbar\omega = 3\hbar\omega_0$, etc. It should be noted that these so called higher harmonics are special cases of two, three, etc. phonon processes.

Fig. 1 shows the scattered neutron intensity as a function of the neutron energy transfer for three temperatures: $T = 15$, 300 and 500 K. At the low temperature, $T = 15$ K, only the side bands above the localized frequency peak and its harmonics are observed. This reflects the fact that at low temperatures only creation of phonons is possible. As the temperature increases, bands appear on both sides of the localized frequency peak, indicating phonon creation and phonon annihilation processes. At the higher energy side band, one local mode and one band mode phonons are mainly created while at the lower energy side band one local mode phonon is created simultaneously with the annihilation of one or more band mode phonons. Similar processes occur at the harmonics of the localized frequency positions but in these cases, at least three phonons at $\hbar\omega = 2\hbar\omega_0$ and four phonons at $\hbar\omega = 3\hbar\omega_0$ participate in the scattering. At elevated temperatures, $KT \gg \hbar\omega_0$, the intensity due to the undesirable phonon processes exceeds the intensity of the one phonon process. This should be more important in cases where there are low frequency local modes.

Fig. 2 shows the same plots for three values of the localized frequency distribution widths. For narrow distributions, the multiphonon contribution is very small but gradually rises as the width increases. This is due to the fact that the height of the localized frequency peak decreases as the width increases while the height of the side band remains constant. It is interesting to note that for large widths, as for the FWHM = 10 meV case, the peaks due to higher harmonics as well as the corresponding shoulders become increasingly wider. This spread increases more rapidly with temperature (see Fig. 1). The fundamental local mode however, apparently decreases only in intensity and is superimposed to the higher order phonon spectrum. Fig. 3 shows the variation of the multiphonon contribution for three hydrogen to metal mass ratio $\mu = M_H/(M_H + M_M) \sim M_H/M_M$. As μ increases, the multiphonon component increases. This would be particularly important in systems where the mass of the atoms others than hydrogen are comparatively small, as for the case of hydrocarbon molecules. In Fig. 4 one can observe the effect of increasing the final neutron energy in a hypothetical experiment carried out at small scattering angles with a metal hydride having two localized frequencies, $\hbar\omega_1 = 127$ meV and $\hbar\omega_2 = 150$ meV. The peak at $\hbar\omega_2$ appears to be superimposed on the side band due to the peak at $\hbar\omega_1$. As the final neutron energy is increased, the magnitude of the scattering vector decreases according to the Eq. (9) for $\theta = 0$. At sufficiently high neutron energy, in the present case at 1000 meV, the side bands

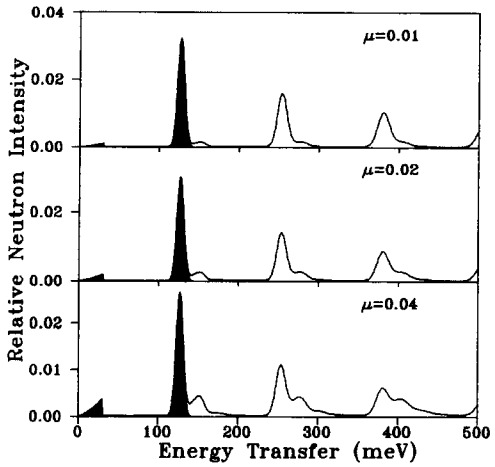

Fig. 3. Calculated relative neutron intensity as a function of the energy transfer in a neutron energy loss scattering experiment with metal hydride for various hydrogen to metal mass ratios. Shaded areas: one phonon scattering. Line: all phonon scattering. $\hbar\omega_0 = 127$ meV, $\omega_D = 30$ meV, $T = 15$ K, $\beta = 10$ meV, $E_f = 4$ meV.

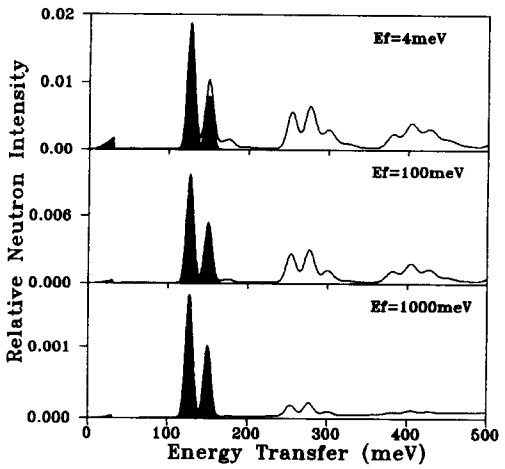

Fig. 4. Calculated relative neutron intensity as a function of the energy transfer in a neutron energy loss scattering experiment with metal hydride for various final neutron energies. Shaded areas: one phonon scattering. Line: all phonon scattering. $\hbar\omega_1 = 127$ meV, $\hbar\omega_2 = 150$ meV, $\omega_D = 30$ meV, $T = 15$ K, $\beta = 10$ meV, $\mu = 0.04$. (Note the decrease of the vertical scales).

are absent around the fundamental transitions but not at the double or triple harmonic. This effect arises because the magnitude of the scattering vector increases as a function of the energy transfer. At the fundamental transition the scattering vector is small and the side bands are negligible but at higher harmonics the scattering vector is large enough for the multiphonon components to be visible. The drastic decrease in the scattering probability at high neutron energies is also apparent.

Comparing the results of the calculations with the experimental data of inelastic neutron scattering on chromium, molybdenum and nickel hydrides[7], one can verify that the shape of the calculated curve in Fig. 1 is very similar to the experimental results, particularly to the data from chromium hydride at 15 K (see Fig. 1 of ref. [7]). This indicates that most of the features due to multiphonon scattering discussed above are present in the experimental results of ref. [7]. The calculated curve also reproduces quite well the shape of the experimental curve at relatively high energy transfer as that due to the third harmonic transition ($\hbar\omega \sim 400$ meV). This result is very difficult to be obtained with the conventional phonon expansion method for, in this case, the expansion must be evaluated at least up to the fourth order term.

5. Conclusions

An alternative way for calculating the multiphonon contribution to the inelastic scattering of neutrons is presented which easily takes into account the multiple phonon processes. The method has been applied to a simple metal hydride system, but could also be applicable to more complex systems as hydrocarbon molecules.

Acknowledgements

Part of this work was sponsored by the International Atomic Energy Agency under the research contract No. 5960/RB.

References

[1] A.I. Kolesnikov, E.L. Bokhenkov and E.F. Sheka, Sov. Phys. JETP 57 (1983) 1270.
[2] R. Hempelmann, D. Richter, O. Hartmann, E. Karlsson and R. Wäppling, J. Chem. Phys.90 (1989) 1935.
[3] S. Ikeda and N. Watanabe, J. Phys. Soc. Japan. 56 (1987) 565.
[4] W. Marshall and S.W. Lovesey, Theory of Thermal Neutron Scattering (Clarendon, Oxford, 1971).
[5] G. Blaesser, J. Peretti and G. Toth, Phys. Rev. 171 (1968) 665.
[6] P. Schofield, Phys. Rev. Let. 4 (1960) 239.
[7] B. Dorner, I.T. Belash, E.L. Bokhenhov, E.G. Ponyatovsky, V.E. Antonov and L.N. Pronina, Solid State Commun. 69 (1989) 121.